Estimation of Equivalent Conicity from Contactless Measurements of Wheel and Rail Profiles

L. Pugi[2] , L. Bocciolini[1],F. Piccioli[1], D. Massini[1], G. Cherici[2], L. Lo Scalzo[2] ,

[1]Italcertifer SPA Piazza della Stazione, 45 - 50123 Firenze, Italia
[2] Università degli Studi di Firenze, Dept. Of Industrial Engineering, Via di Santa Marta 3, 50139 Firenze, Italia, luca.pugi@unifi.it orcid id https://orcid.org/0000-0001-7385-9471

Abstract. Measurement of Equivalent Conicity is quite important index to properly evaluate geometric quality of rails and wheels. The way in which this index is evaluated is evaluated is described by the standard EN 15302 from online contactless measurement of rail profiles performed by a dedicated measurement coach. The numerical treatment of large amount of data derived by the acquisition of a huge number of measured rail profiles should be performed with great accuracy but also with a great numerical efficiency to assure a near to real time evaluation of performed analysis. In this work authors describe an efficient procedure developed using open-source software that has been developed to meet accuracy, efficiency, and portability specifications. Paper investigates how different integration and smoothing should affect efficiency and accuracy of performed operations. Proposed approach is first validated on numerical synthetic inputs and then validated on experimental data, also comparing performances of the proposed software with a commercial one. Results are encouraging, demonstrating the feasibility of the proposed approach for the realization of flexible and efficient tools for Real-Time implementation of the estimation of equivalent conicity for railway applications.

1. List of adopted Symbols

y, y_0=transversal motion of the axle respect to rails (pedex 0 is used to describe the initial value of the transversal displacement of the axle respect to rails);
r, r_0=rolling radius of wheels (pedex 0 is used to identify nominal value associated to a null lateral displacement);
b_a= half track;
γ, γ_e=conicity and equivalent conicity;
ω_k, λ=hunting frequency and period;
x,v= longitudinal displacement and speed of the axle;
δx=integration step;
N_{sample}=scaling factor adopted to evaluate the integration step
Ψ=derivative of transversal motion y respect to longitudinal motion x

2. Introduction: definition of equivalent conicity and its measurement

Stability and safety of railway vehicles is strongly influenced by the geometry of wheel-rail contact. A fundamental background to understand these phenomena is represented by the so called “Klingel model” as stated by fundamental text and handbooks of railway vehicle dynamics[1],[2].
Klingel approach is described by the scheme of figure 1: a wheelset with constant conicity γ is coupled with rails that are modelled as straight linear elements with negligible transversal dimensions

(substantially two blades) so the position of the contact on rails is substantially assigned. This ideal conical rigid axle is studied considering an ideal kinematic behaviour in which pure rolling conditions are always verified. According to Klingel model the kinematic behaviour of a free axle over rails is described by equation (1):

$$\frac{d^2y}{dx^2}+\frac{\Delta r(y)}{2b_A r_0}=0 \Rightarrow \frac{d^2y}{dx^2}+\frac{2\tan(\gamma)y}{2b_A r_0}=0 \Rightarrow y\tan\gamma + r_0 b_a \frac{d^2y}{dx^2}=0 \tag{1}$$

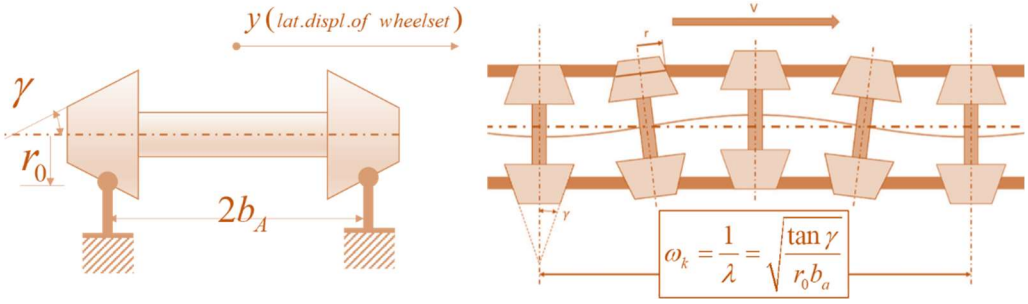

Figure 1. Klingel model [1],[2].

Free response of the wheelset according to differential equation (1) is described by a sinusoidal solution respect to travelled space x, whose frequency ω_k can be calculated according to equation (2)

$$\omega_k = \frac{1}{\lambda} = \sqrt{\frac{\tan\gamma}{r_0 b_a}} \tag{2}$$

Klingel model is a simple explanation of a more complex behaviour of real wheel and speed profiles which have a shape that is clearly optimized respect to different specifications regarding loading capability, stability, durability etc.

However, for a known couple of wheel and rail profiles is still possible to calculate a $\Delta r(y)$ function which describes the variation of the rolling radius of both wheels respect to a transversal displacement y (this is clearly simpler in the hypothesis of a single contact for each wheel).

In this hypothesis ideal kinematic interaction between a free axle and rails is still describe by equation (1) however since $\Delta r(y)$ is a nonlinear function of the transversal displacement y the solution is still periodic, but it's not associated to a pure sinusoidal motion with the constant frequency ω_k described by equation (2) but to a periodic motion whose period $\lambda(y_0)$ is a function of the considered initial value of the transversal displacement y_0 In particular $\lambda(y_0)$ is calculated assuming a null initial value of the derivative of y (dy/dx).

Since $\lambda(y_0)$ is variable is possible to define an equivalent conicity $\gamma_e(y_0)$ according to (3) as the equivalent constant conicity that should produce according Klingel model a sinusoidal motion with the same period.

$$\gamma_e(y_0) = \tan^{-1}\left(\frac{r_0 b_a}{\lambda^2}\right) \tag{3}$$

Equivalent conicity play a key role in determining important features of the interaction between axles and rails. In particular according literature [2] higher values of equivalent conicity assure a good steering capacity of the axle respect to involved transversal displacement. However also hunting frequencies of the axles increase with γ_e, so high level of conicity has negative effects on the stability of the vehicle exciting undamped poles/frequencies of the system and causing a potential reduction of vehicle critical speed. For this reason, geometric matching between wheel and rail profiles must be carefully evaluated for its potential consequences on vehicle performances and safety. For this reason specific railway standards such as as EN15302[3] describe the way in which this kind of measurements should be performed.

Recent studies prove a strong correlation between measured conicities and measured lateral accelerations[4] so this contactless measurement is strongly correlated to ride dynamics quality.

More generally even very recent publications [5-6] still consider the evaluation of equivalent conicity as a fundamental parameter to properly investigate state and stability of railway vehicles

Equivalent conicity cannot be directly measured since it's a derived from the solution of equation (2) that can be performed only if the function $\Delta r(y)$is known from the measurement of both wheel and rail profiles. For this reason, the typical measurement layout described in figure 2 and adopted by Italcertifer is composed by the following elements:

- A laser scanner system able to measure accurately both rail profiles. Since a rail profile is acquired every 25 cm of travelled distance amount of acquired data and precision of performed measurements is a quite critical aspect.
- An accurate geo-referencing system able to identify vehicle position and kinematics from GPS IMU measurement integrated with encoder measurements of wheel speed/rotation. This is a typical approach of odometry and railway localization systems [8].
- Wheel profiles should be considered as relatively stable constant for travelled distance of less than 1000km. So, their measurement is typically performed statically with a greater precision that is assured by mechanical callipers and by the repetition of a measurement which is substantially not time constrained.
- All these data are then acquired and post-processed by a computational platform (typically a work-station) able to perform the calculation of equivalent conicity as described in equations (1-3). This calculation must be resilient against measurement errors especially on contactless measurements of rail profiles, so also some filtering/smoothing techniques must be implemented.

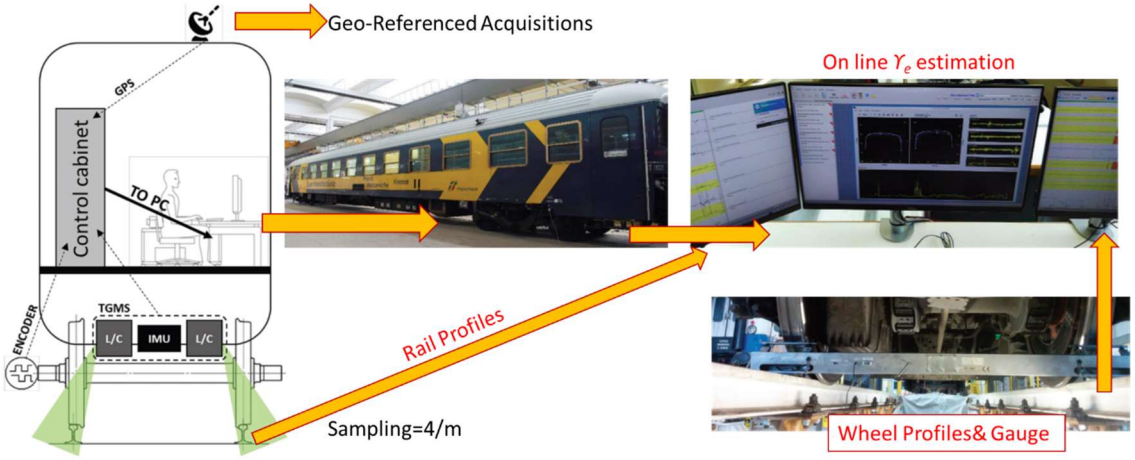

Figure 2. Contactless measurement system of equivalent conicity adopted by Italcertifer[4].

Currently these measurements and analysis are performed by specialized commercial tool with limited level of customization, high costs, a substantially null possibility of verifying and autonomously assessing the way in which data are treated.

Aim of this work is to propose an open tool for the evaluation of equivalent conicity from online measurement. Aim of the tool is not only a mere reduction of costs which are not very important respect to the overall value of performed tests, but to produce a tool that can be easily customized for different calculation platforms to also meet the possibility of an overall real time implementation of the system.

For this reason the proposed tool is developed using Python, a free progamming language commonly adopted for scientific calculations.

This is a possibility that is not trivial considering the involved high sampling frequency of acquired profiles and the necessity of producing accurate estimation according to specifications that are clearly indicated in reference standards [3]. Also, development with an open platform offers the possibility of defining common procedures that can be easily shared, inspected, and verified by different structures involved not only in the development but also in verification and validation of developed tools. A complete re-implementation of the postprocessing software also offer the occasion to evaluate how different approaches to the problem can lead to more robust or efficient implementations of the problem.

The discussion is organized as follows:

- Evaluation of different integration/solution methods in terms of numerical efficiency and robustness;

- Calibration of Smoothing and Filtering of input data with synthetic data.
- Cross Validation of implemented tool by comparing the results of proposed tool with an homologated commercial software on the same input experimental data provided by Italcertifer SPA.

3. Robust Evaluation of Equivalent Conicity

For the evaluation of equivalent conicity is first necessary to evaluate the behaviour of the function $\Delta r(y)$ this is not the most consuming activity in terms of involved numerical resources and for its implementation are available different methods [9-11] which are all fundamentally implemented from the original work of Shabana[9].
Once the $\Delta r(y)$ is evaluated equivalent conicity for each value of initial displacement y_0 must be evaluated; According regulations in force four different methods should be adopted [3], however the same standards strongly recommends the first two methods which are substantially related to a numerical solution of equation (2):

- Direct Integration:equation (2) is directly integrated and the period of simulated oscillation is evaluated to directly calculate period λ and consequently equivalent conicity γ_e;
- Double Integration method: it's a two step integration method ;to directly calculate the amplitude of the performed oscillation;

3.1. Direct Integration

For a known constant value of conicity γ the shape of the sinusoidal solution of (2) is known.
The value of the local conicity
For a small variation of the transversal displacement y a local value of conicity γ can be calculated from $\Delta r(y)$ according (4)

$$2\tan\gamma \approx \frac{\Delta r(y)}{y} \tag{4}$$

Then knowing the initial displacement y_0 and its derivative it is possible to calculate iteratively the solution for each intermediate n^{th} step y_n according to (5)

$$\begin{aligned} y_{n+1} &= y_n \cos\left(\omega_k(y_n)dx\right) + \frac{1}{\omega_k(y_n)}\frac{dy_n}{dx}\sin\left(\omega_k(y_n)dx\right) \\ \frac{dy_{n+1}}{dx} &= -y_n\omega_k(y_n)\sin\left(\omega_k(y_n)dx\right) + \frac{dy_n}{dx}\cos\left(\omega_k(y_n)dx\right) \end{aligned} \tag{5}$$

This approach apparently interesting, is substantially not very useful for a fast, robust implementation since the implementation of sinusoidal functions is computational very expensive, also the implementation should be affected by numerical troubles especially when extremely high or extremely low values of equivalent conicity are recorded.
For both this reason this method was substantially discarded in favour of a general approach based on the so-called State Space representation of the system (6).

$$\frac{d^2y}{dx^2} + \frac{2\tan\left(\gamma(y)\right)y}{2b_A r_0} = 0 \Rightarrow \begin{bmatrix} \frac{dy}{dx} \\ \frac{d^2y}{dx^2} \end{bmatrix} = \overbrace{\begin{bmatrix} 0 & 1 \\ \frac{\tan\left(\gamma(y)\right)}{b_A r_0} & 0 \end{bmatrix}}^{A} \begin{bmatrix} y \\ \frac{dy}{dx} \end{bmatrix} \tag{6}$$

Equation (6) can be directly integrated one of the classical fixed step integrator algorithms[12] such as Euler Method (also known as ODE1) or Heun one (also known as ODE2 or trapezoidal rule).
Optimization of the integration step δx for a fixed step solver should pose some problems since integration process is performed on measured wheel and rail profiles so behaviour of the integrated function (6) should be quite variable. The solution to this trouble should be the adoption of solvers/integrators with both variable step and order that should automatically perform the optimization

of integration parameters[14]. However, authors preferred a customized solution based on the adoption of a fixed order integrator with a variable integration step that is scheduled before the integration of (6): function $\Delta r(y)$ is pre-calculated and known before the integration of equation (6) so for each value of y, eigenvalues/frequencies $\omega_k(y)$ respect to transversal position y are known. Integration step δx is then calculated as inversely proportional to local value of $\omega_k(y)$ according (7) through a scaling factor N_{sample} that should be calibrated to obtain the desired trade-off between accuracy and involved numerical resources

$$\delta x = \frac{1}{\omega_k(y) N_{sample}} \tag{7}$$

Accuracy of proposed integration methods is tested on benchmark wheel and rail profiles that are provided by the same standard EN15302 which provide a wide population of wheel and rail profiles that have been fully exploited to perform verification activities of the proposed methodology. However in this work authors have shown results which are substantially referred to two different wheel profiles (A and H according to EN15302) and single rail one (rail A according to EN15302). Wheel and rail profiles considered in this work are shown in figures 3,4 and 5.

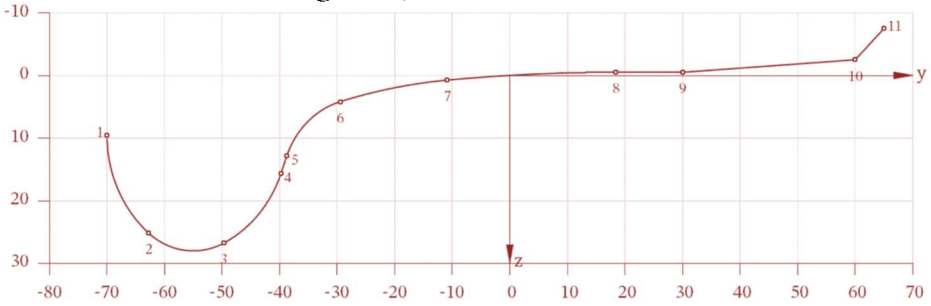

Figure 3 Wheel profile A [3]

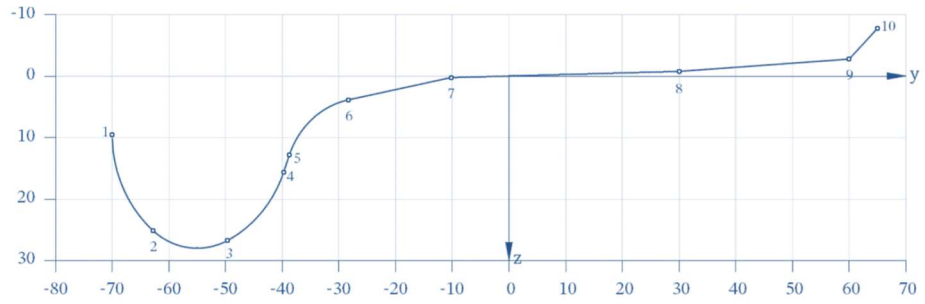

Figure 4 Wheel profile H [3]

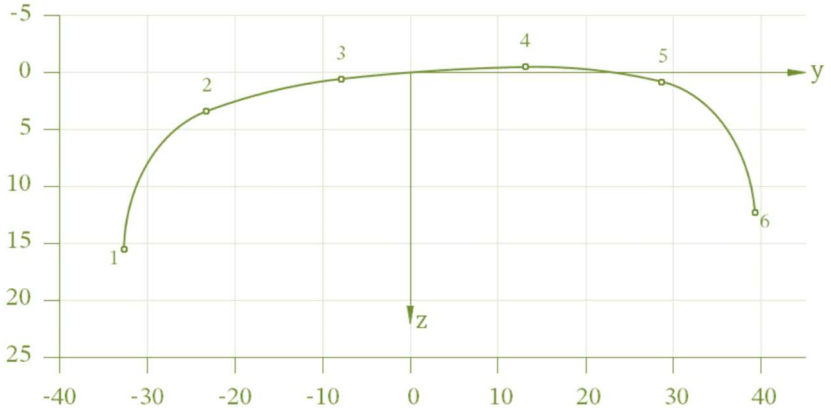

Figure 5 Rail profile A[3]

For chosen profiles $\gamma_e(y_0)$ is calculated by integrating (6) and assuming different values of initial displacement y_0 (each spaced of 0.1mm);

Regulations in force [3] define for each couple of benchmark rail and wheel profile a reference $\gamma_e(y_0)$ and an interval of admissible errors tolerances. For wheel profile "A" rail one "A" these curves are shown in figure 6 and are compared with corresponding results of the overcited integration of (6) performed respectively with different fixed step integrators (first order Euler or second order Heun). In the same graph it is also evaluated the computational time needed to execute performed calculations referred to a single thread/core implementation on an I7 processor.
Resulting integration time is substantially proportional to the parameter N_{sample} ; only for very low value of N_{sample} (N_{sample} <500) this proportionality is not respected since the maximum integration step is saturated to a maximum value that cannot be superated.
Results clearly shows that an increased order of the integrator is substantially convenient especially when large integration steps are adopted since obtained solutions are smoother and more accurate with limited or negligible increase of computational time. Also, for finer integration steps the second order integrator assures much smoother solutions with a relatively modest increments of computational loads.
This comparison between different integrators is repeated also for the wheel profile "H" coupled with the same "A" rail profile: results limited to a value of $N_{samples}$ equal to 500 are shown in figure 7.

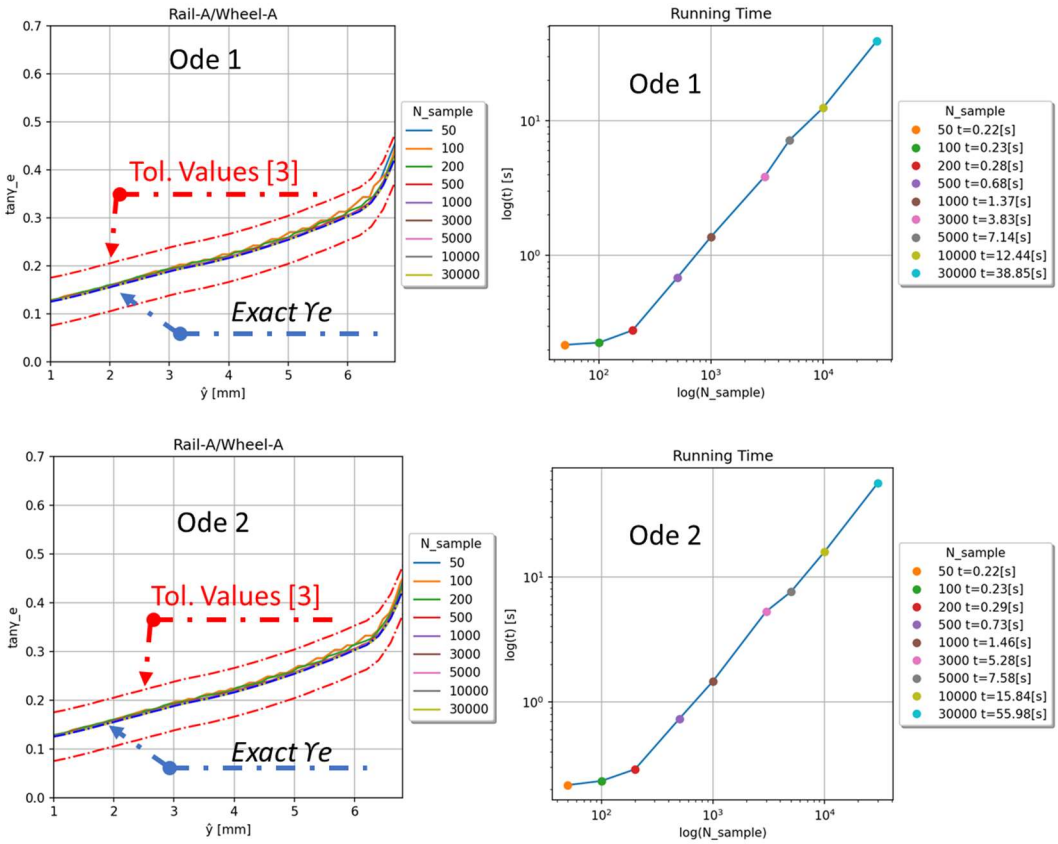

Figure 6 Comparison of achieved performances with ODE 1 (euler) and ODE 2(euler) for wheel profile A and rail profile A[3]

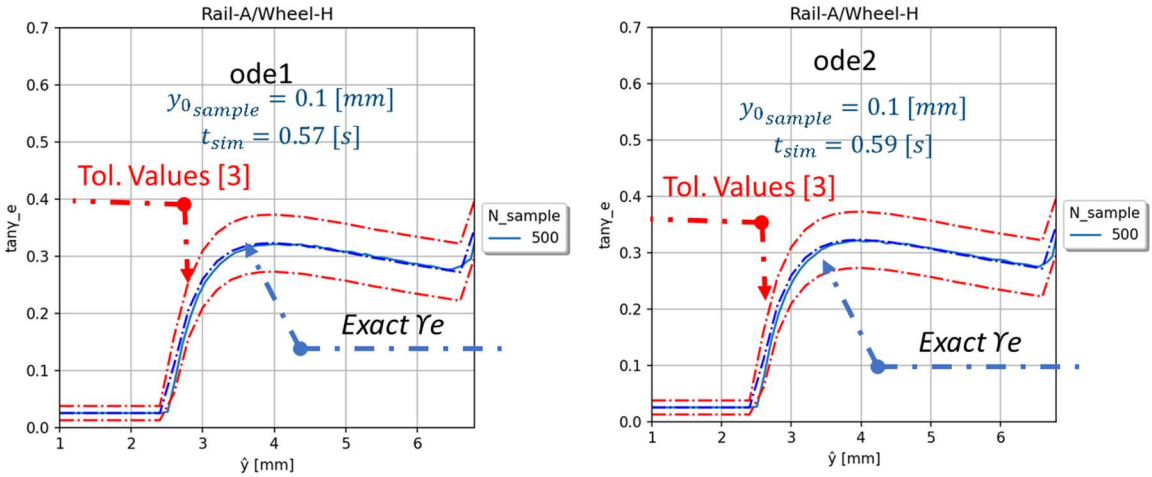

Figure 7 Comparison of achieved performances with scheduled ODE 1 (euler) and scheduled ODE 2(euler) for wheel profile A and rail profile H[3] limting the analysis to a constant fixed sampling of 500 points (a sampling of 0.014[mm])

The shape of $\gamma_e(y_0)$ is different respect to the previous case but the advantage of the higher order integrator is confirmed; Also computational time for a single core implementation is quite encouraging since about 0.6 seconds are needed for the complete evaluation of a profile. Considering that a profile is acquired every 0.25 meter of travelled distance, the corresponding sampling frequency in time domain is proportional to vehicle speed ranging from about 60 to 200Hz for a train speed from 50 to 200kmh. Current code is implemented for a parallel execution so the real execution time of the code should be evaluated as the ratio between the elapsed time need to elaborate an acquired conicity profile and the number of parallelized threads that are available for the calculation. So numerical configurations of figure 7 (ode1-ode2 $N_{samples}$=500) is better suited for a fast postprocessing which is still slower than Real Time especially if it is considered the implementation on a low-cost commercial workstation since, as example, the current number of threads for a I9 processor is around 32-36[13].
However Authors are quite confident that dispatching the calculation to more than a processor, and exploiting both lower values values of $N_{samples}$ and the increased performances of more recent CPUs an hard real time implementation is potentially possible.

3.2. Double Integration method

It is possible to define the gradient ψ according (8) and then rewrite equation (6) respect to ψ obtaining equation (9).

$$\psi = \frac{\dot{y}}{\dot{x}} = \frac{dy}{dx} \tag{8}$$

$$\psi d\psi = -\frac{\Delta r(y)}{2b_A r_0} dy \tag{9}$$

Equation (9) can be integrated respect to y obtaining $\psi(y)$ as described by (10):

$$\frac{1}{2}\left(\psi^2(y) - \psi^2(y_{\min})\right) = -\frac{1}{2b_a r_0}\int_{y_{\min}}^{y} \Delta r(y)\,dy \Rightarrow \psi(y) = \sqrt{\frac{1}{b_a r_0}\int_{y_{\min}}^{y} \Delta r(y)\,dy} \tag{10}$$

Where $\begin{cases} \psi(y_{\min}) = 0 \\ \psi(y_{\max}) = 0 \end{cases}$

In particular gradient ψ calculated by (10)is null when maximum (y_{max}) and minimum (y_{min}) values of lateral motion y are reached.

Period λ of performed oscillations can be calculated by further integrating the gradient ψ between y_{min} and y_{max} according (11)

$$dx = \frac{1}{\psi(y)}dy \Rightarrow \lambda(y_{min}) = 2\int_{y_{min}}^{y_{max}} \frac{1}{\psi(y)}dy \tag{11}$$

Also for the double integration method different solver/integrator are tested but at the end as in the case of direct integration but at the end the more convenient way to solve the system is to use a schedule step solver with fixed order. For what concern involved numerical resources at the end double integration and direct integration methods are almost equivalent. All these consideration are roughly summarized in the graph of figure

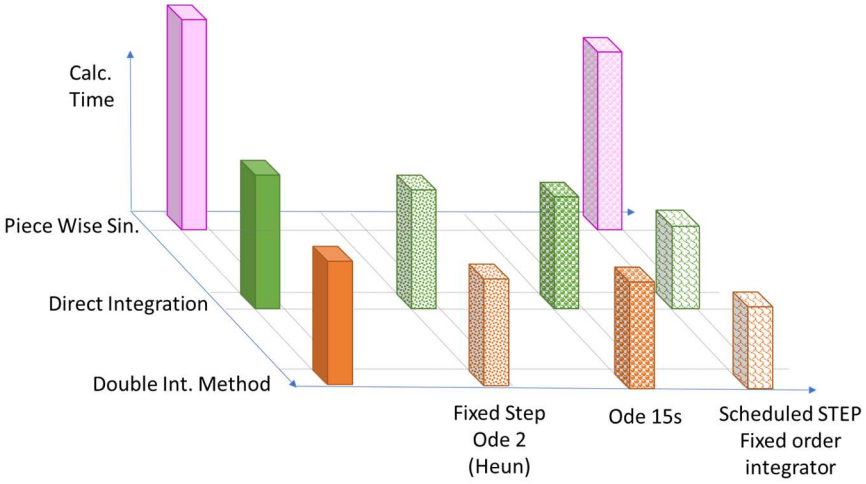

Figure 8 final comparison of different methods and integrators in terms of involved computational resources

4. Smoothing of Acquired Profiles

Acquired Rail profiles are affected by noise that is substantially unavoidable for the dynamic nature of performed measurement. As visible in figure 9, acquired profiles are substantially clouds of points perturbed by a gaussian noise. This noise should have negative effects on accuracy of performed results so acquired profiles must be smoothed.

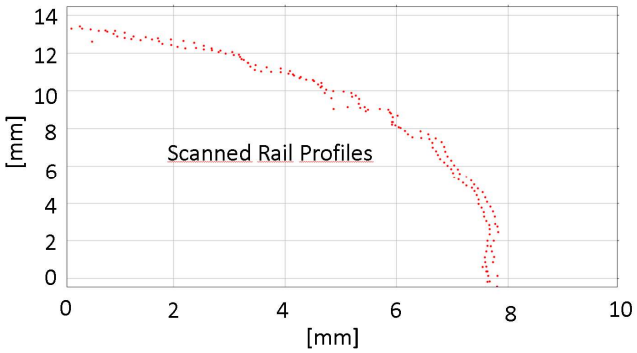

Figure 9 final comparison of different methods and integrators in terms of involved computational resources

To evaluate and calibrate different smoothing filters ideal and perturbed profiles should be available; unfortunately, on available experimental results only perturbed profiles are available.
So, authors decided to compensate this trouble adopting the following procedure:

- Preliminary Calibration on Synthetic Input: syntethic clouds of ponts are produced by adding a gaussian noise (variance of about 0.1mm)
- Cross-Validation with another commercial software: real experimental data are provided as input to proposed tool (including tested smoothing filters) and a known validated commercial software verifying a substantial equivalence of obtained results. This is only a cross validation since this test only demonstrates only that proposed tool has performances that are substantially aligned to most performing commercial tools, maintaining its fundamental advantages respect to other product in terms of costs, flexibility, numerical performances.

4.1. Preliminary Calibration on Synthetic Input

In figure 10 it is shown an example of synthetic perturbed input

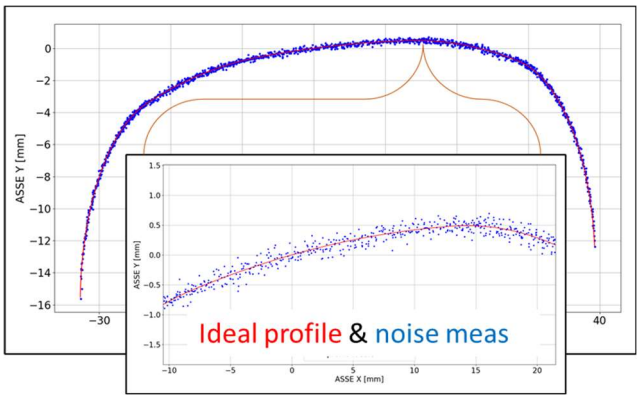

Figure 10 example of synthetic input to calibrate

To properly calibrate and evaluate the quality of a smoothing filter it's possible to define some statistic indexes such of the error between ideal profile and the perturbed one after filtering, such as mean error, standard deviation, statistical distribution of errors (95th percentile). In this way various kind of filters have been iteratively calibrated trying to minimize the error on reconstructed profiles.
In figure 10/a it's shown an example of performed optimization of a running mean filter: it's interesting to notice that there is a value of the calibration parameter (size of the window in terms of samples on which is performed the running mean) for which all the indexes that describe errors on smoothed profiles are minimized. Unfortunately comparing these results with corresponding behaviour of errors on calculated γ_e, a weak correlation is found: errors on estimated γ_e decrease for calibration that apparently produce a sub-optimal optimization of the filtered profile. Comparison is then repeated considering as filtering index the derivative of errors on reconstructed rail profiles respect to the transversal displacement y. As visible in figure 10/b,this second index is then compared to errors on estimated γ_e showing a much better correlation. It should be concluded that for the calibration of smoothing filters is not very important to properly reconstruct the exact profiles but its derivatives respect to y. This interesting result can be understood considering that equivalent conicity is substantially influenced by a proper calculation of the $\Delta r(y)$ function that is strongly influenced by gradients along y of the rail profiles. In this way this is also an indirect confirmation of the adopted integration method with an integration step δx that is scheduled respect to local local eigenvalues and consequently respect to $\Delta r(y)$.

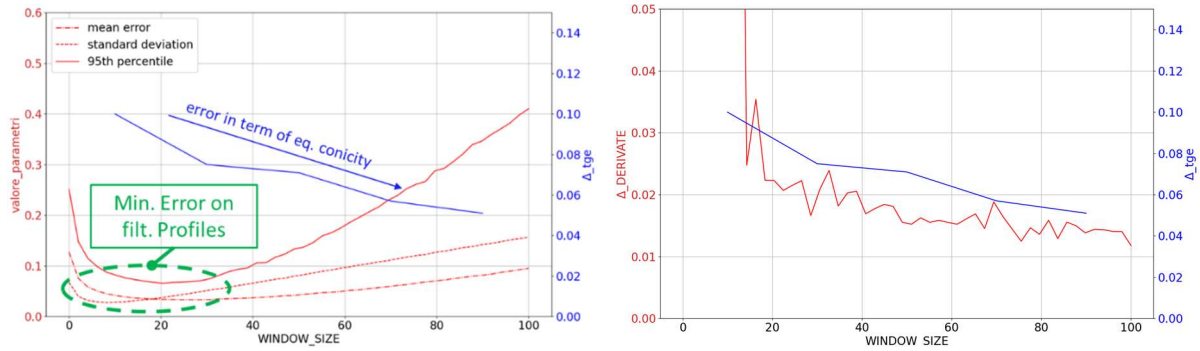

a) b)

Figure 11/a/b example of calibration of a running mean filter (window size on which is performed the running mean), comparing error on estimated γ_e respect to various error indexes on profiles s (a) and derivatives (b)

For what concern the list of evaluated smoothing filters authors decided to investigate quite different approaches and solutions:

- Running Mean/Uniform Filter: the simplest digital filter in which a running mean of measured values is performed over a fixed window.
- Gaussian Filter: since applied noise on synthetic input, this filter should be surely favourited[15] .
- Savitzky–Golay filter[16][17][18]: it is a least-squares polynomial smoothing filter that is often proposed in literature for similar applications.
- Interpolating Curve-Filters:
    - Chebyshev Poly[19]
    - Spline with smoothing[20]

In Table I it is shown a brief comparison between investigated filters according the over introduced performance indexes. Also, the computational time to perform the filtering of 10000 profiles.
According results of Table I, most interesting performances are assured by the running mean filters with assure not only the lower error in terms of calculated conicity but also the lower computational time. Considering the hypothesis of a gaussian noise on measurements these results was quite unexpected.

Table I: Comparison between different filters in terms of various performance indexes

Filter Type	Mean Error [mm]	Standard Deviation [mm]	95th Perc.Error [mm]	Errors on Derivative	$\Delta tg\gamma_e$ Error on Est.Conicity	Time [s/10000Run]
uniform	0.0616	0.1133	0.2391	0.0154	0.0445	0.39
gauss	0.0337	0.0514	0.0822	0.0182	0.0681	1.74
Sav-Gol	0.0288	0.0304	0.0699	0.0170	0.0514	10.38
cheby	0.1049	0.1068	0.2714	0.0176	0.0652	16.40
spline	0.0649	0.0597	0.1415	0.0285	0.1932	61

4.2. Cross Validation on Experimental Data

The entire tool (smoothing filter and integrator) is tested using experimental data that are recorded on the Campiglia-Grosseto line visible in figure 12. Tests are performed on an instrumented coach with a

wheel diameter of 920mm and a wheel profile S1002. The length of the line is about 20km (corresponding to about 80000 acquired rail profiles), nominal rail profiles are S100.
Same input data are provided to a commercial tool, that is widely accepted and verified, comparing the estimated equivalent conicity provided by the proposed tool and the commercial one.
As visible in figure 13, where the cumulative distribution of errors between the two software is shown, there is a substantial equivalence on performed measurements so it is possible to conclude that at least proposed tool is equivalent to commercial one for what concern the accuracy of estimated conicity on experimental data.

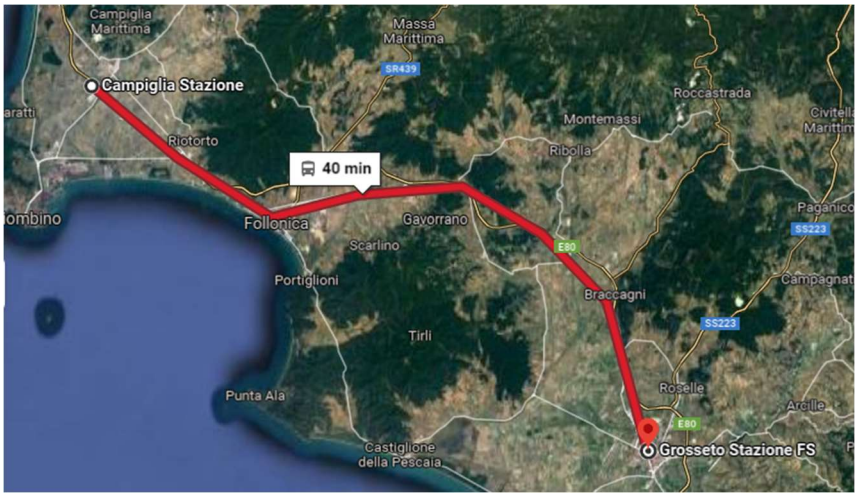

Figure 12 Test Railway Line (CAMPIGLIA-GROSSETO), length of 20km, about 80000 rail profiles, (Wheel Profile S1002, diameter 920 mm Rail S100)

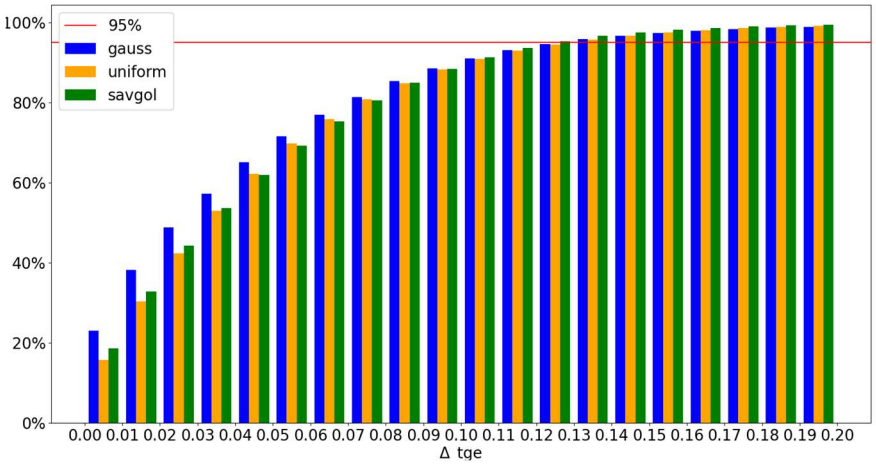

Figure 13 Cumulative distribution of differences in terms of $\Delta\tan\gamma_e$ between investigated tool and a commercial reference one.

5. Conclusions and future Developments

In this work it is proposed an open tool developed in Python that have been successfully used to evaluate the equivalent conicity line according to regulations in force [3]. Proposed tool has been cross-validated by comparing its performances in terms of accuracy with an existing commercial software. However, the proposed tool has very appetible features respect to this existing solution in terms of scalability, numerical performances and more generally traceability of operations that are really performed on acquired data. A non secondary contribution of the activity was also the possibility of extensively verify

different implementation techniques also proposing some innovative contributions for what concern, as example the way in which equations of the proposed estimator are iintegrated.
Activities on proposed tools will prosecute extending the validation set of experimental data. In particular it should be interesting to perform some further measurements on rails with more precise instruments (as example static measurements performed with different sensors) to further calibrate and assess the precision of the proposed tool.
For what concern future Real Time implementation authors are quite confident that a further improvement of tool in term of numerical efficiency should be obtained exploiting tools and knowledge deriving from a consolidated series of applications developed in last 20 years[21-25].

6. References

[1] ESVELD, Coenraad; ESVELD, Coenraad. Modern railway track. Zaltbommel: MRT-productions, 2001.

[2] WICKENS, A. H. A history of railway vehicle dynamics. In: Handbook of railway vehicle dynamics. CRC Press, 2019. p. 5-42.

[3] EN 15302 September 2019Railway Applications - Wheel-rail contact geometry parameters – Definitions

[4] Massini, D., Pugi, L., Bocciolini, L., Piccioli, F., Zappacosta, C. Experimental investigation on stability and equivalent conicity of a rolling stock [Analisi sperimentale sulla stabilità e la conicità equivalente di un rotabile ferroviario] (2020) Ingegneria Ferroviaria, 75 (5), pp. 333-347.

[5] Saba, E., Kalwar, I.H., Unar, M.A., Memon, A.L., Pirzada, N. Fuzzy logic-based identification of railway wheelset conicity using multiple model approach (2021) Sustainability (Switzerland), 13 (18), art. no. 10249, . DOI: 10.3390/su131810249.

[6] Shabana, A.A. Geometric self-centering and force self-balancing of railroad-vehicle hunting oscillations (2021) Acta Mechanica, 232 (8), pp. 3323-3329. DOI: 10.1007/s00707-021-02983-w

[7] Attivissimo, F., Danese, A., Giaquinto, N., Sforza, P. A railway measurement system to evaluate the wheel-rail interaction quality (2007) IEEE Transactions on Instrumentation and Measurement, 56 (5), pp. 1583-1589. DOI: 10.1109/TIM.2007.903583

[8] Allotta, B., D'Adamio, P., Malvezzi, M., Pugi, L., Ridolfi, A., Vettori, G. A localization algorithm for railway vehicles (2015) Conference Record - IEEE Instrumentation and Measurement Technology Conference, 2015-July, art. no. 7151350, pp. 681-686. DOI: 10.1109/I2MTC.2015.7151350

[9] SHABANA, Ahmed A., et al. On the computer formulations of the wheel/rail contact problem. Nonlinear Dynamics, 2005, 40.2: 169-193.

[10] Meli, E., Malvezzi, M., Papini, S., Pugi, L., Rinchi, M., Rindi, A. A railway vehicle multibody model for real-time applications (2008) Vehicle System Dynamics, 46 (12), pp. 1083-1105. DOI: 10.1080/00423110701790756

[11] Liu, H., Yu, Z., Guo, W., Jiang, L., & Kang, C. (2019). A novel method to search for the wheel–rail contact point. International Journal of Structural Stability and Dynamics, 19(11), 1950142.

[12] FATHONI, Muhammad Faris; WURYANDARI, Aciek Ida. Comparison between Euler, Heun, Runge-Kutta and Adams-Bashforth-Moulton integration methods in the particle dynamic simulation. In: 2015 4th International Conference on Interactive Digital Media (ICIDM). IEEE, 2015. p. 1-7.

[13] https://en.wikipedia.org/wiki/List_of_Intel_Core_i9_processors

[14] Shampine, L. F., M. W. Reichelt, and J.A. Kierzenka, "Solving Index-1 DAEs in MATLAB and Simulink," SIAM Review, Vol. 41, 1999, pp. 538–552.

[15] Yun, T., Jiang, K., Li, G., Eichhorn, M. P., Fan, J., Liu, F., ... & Cao, L. (2021). Individual tree crown segmentation from airborne LiDAR data using a novel Gaussian filter and energy function minimization-based approach. Remote Sensing of Environment, 256, 112307.

[16] Chen, J., Jönsson, P., Tamura, M., Gu, Z., Matsushita, B., & Eklundh, L. (2004). A simple method for reconstructing a high-quality NDVI time-series data set based on the Savitzky–Golay filter. Remote sensing of Environment, 91(3-4), 332-344.

[17] SCHAFER, Ronald W. What is a Savitzky-Golay filter?[lecture notes]. IEEE Signal processing magazine, 2011, 28.4: 111-117.
[18] Savitzky, A.; Golay, M.J.E. (1964). "Smoothing and Differentiation of Data by Simplified Least Squares Procedures". Analytical Chemistry. 36 (8): 1627–39. Bibcode:1964AnaCh..36.1627S. doi:10.1021/ac60214a047
[19] HIBINO, Masao; ISHIZAKI, Yasutoshi; WATANABE, Hitoshi. Design of Chebyshev filters with flat group-delay characteristics. IEEE Transactions on circuit theory, 1968, 15.4: 316-325.
[20] Rodriguez, German (Spring 2001). "Smoothing and Non-Parametric Regression" (PDF). 2.3.1 Computation. p. 12. Retrieved 28 August 2017
[21] Pugi, L., Malvezzi, M., Tarasconi, A., Palazzolo, A., Cocci, G., Violani, M.HIL simulation of WSP systems on MI-6 test rig (2006) Vehicle System Dynamics, 44 (SUPPL. 1), pp. 843-852. DOI: 10.1080/00423110600886937
[22] Locorotondo, E., Pugi, L., Berzi, L., Pierini, M., Lutzemberger, G.Online Identification of Thevenin Equivalent Circuit Model Parameters and Estimation State of Charge of Lithium-Ion Batteries (2018) Proceedings - 2018 IEEE International Conference on Environment and Electrical Engineering and 2018 IEEE Industrial and Commercial Power Systems Europe, EEEIC/I and CPS Europe 2018, art. no. 8493924, . DOI: 10.1109/EEEIC.2018.8493924
[23] Pugi, L., Galardi, E., Carcasci, C., Lucchesi, N.Hardware-in-the-loop testing of bypass valve actuation system: Design and validation of a simplified real time model (2017) Proceedings of the Institution of Mechanical Engineers, Part E: Journal of Process Mechanical Engineering, 231 (2), pp. 212-235. DOI: 10.1177/0954408915589513
[24] Pugi, L., Reatti, A., Corti, F., Grasso, F. A Simplified Virtual Driver for Energy Optimization of Railway Vehicles (2020) Proceedings - 2020 IEEE International Conference on Environment and Electrical Engineering and 2020 IEEE Industrial and Commercial Power Systems Europe, EEEIC / I and CPS Europe 2020, art. no. 9160715, .DOI: 10.1109/EEEIC/ICPSEurope49358.2020.9160715
[25] Pugi, L., Allotta, B. Hardware-in-the-loop testing of on-board subsystems: Some case studies and applications (2012) Railway Safety, Reliability, and Security: Technologies and Systems Engineering, pp. 249-280. DOI: 10.4018/978-1-4666-1643-1.ch011